

## Phase Separation, Density Fluctuation, and Critical Dynamics of N<sub>2</sub> in Aerogel

A. P. Y. Wong,<sup>(1),(a)</sup> S. B. Kim,<sup>(1)</sup> W. I. Goldberg,<sup>(2)</sup> and M. H. W. Chan<sup>(1)</sup>

<sup>(1)</sup>*Department of Physics, Pennsylvania State University, University Park, Pennsylvania 16802*

<sup>(2)</sup>*Department of Physics and Astronomy, University of Pittsburgh, Pittsburgh, Pennsylvania 15260*  
(Received 26 March 1992)

Light scattering was used to study N<sub>2</sub> confined in aerogel. We find evidence of liquid-vapor phase separation that terminates at a critical point. Whereas the width of the coexistence curves is substantially reduced relative to bulk N<sub>2</sub>, the shape of the coexistence curve is similar to that found for the bulk. Photon correlation spectroscopy shows that the density fluctuations decay algebraically in time, a result consistent with the random-field Ising model.

PACS numbers: 64.70.Fx, 64.60.Ht, 75.40.Gb

There have been quite a few recent experiments studying near-critical binary fluid mixtures entrained in random media such as porous glasses [1,2], polymers [3], and silica gels [4]. These experiments are motivated, to a large extent, to look for effects related to the random-field Ising model (RFIM) [5]. Because of the slow kinetics related to mass diffusion and wetting in narrow pores [6] and the difficulty in adjusting the exact critical composition of fluid in the porous medium [2], fundamental questions about the interpretation of the experiments are still not resolved. Most of these experiments found evidence of slow kinetic and history dependence phenomena [1-4]. It is, however, not clear whether these observations are relevant to the RFIM system. The critical dynamics of a RFIM, due to energy barriers introduced by the random fields, are predicted to be governed by an activated [7] process. If the random-field critical point  $T_{c,R}$  is approached from above, the intensity autocorrelation function  $G(\tau)$  which reflects density fluctuation, for example, is expected to decay algebraically with time. For a pure system near criticality, an exponential decay of  $G(\tau)$  is expected.

Recently, two of us [8] reported a heat capacity study of <sup>4</sup>He confined in aerogel of 95% porosity near the critical point of <sup>4</sup>He. This <sup>4</sup>He experiment has an advantage over those involving binary fluid mixtures in that the chemical potential, i.e., the vapor pressure of the system, can be easily tuned. The <sup>4</sup>He experiment shows evidence of liquid-vapor-like phase separation that terminates at a genuine critical point that is 32 mK below bulk  $T_c$ . Heat capacity scans at appropriate fixed fluid density exhibit a small but sharp peak. The position of the peak first increases then decreases with the fluid density. This is suggestive of a liquid-vapor coexistence boundary. What is remarkable is that the coexistence boundary of <sup>4</sup>He in aerogel is fully 14 times smaller than that of bulk <sup>4</sup>He, but the exponent characterizing its shape is  $0.28 \pm 0.05$ , consistent with that of the bulk value but not consistent with the nearly zero value expected for the conventional RFIM [7,9,10].

In this paper we report the results of a light scattering study of fluid N<sub>2</sub> entrained in a piece of aerogel that

came from the same batch as that used in the <sup>4</sup>He study. In addition to confirming the findings of the <sup>4</sup>He heat capacity experiment, namely, the presence of liquid-vapor phase separation, we find strong density fluctuation as the system is lowered from one-phase toward the critical region. We find evidence that the liquid and vapor domains in the coexisting region are "frozen" in size. There is also evidence of activated critical dynamics.

The aerogel sample is shaped and snugly fit inside a Cu cell with a cylindrical interior of 1.06 cm in diam and 0.4 cm in height. Cooling is provided by a liquid nitrogen reservoir that is thermally weakly linked to the sample cell. The temperature of the cell is monitored by a platinum resistance thermometer and regulated to within 3 mK via a negative feedback circuit. The sample cell and the liquid nitrogen reservoir are enclosed in a vacuum chamber. The average density of N<sub>2</sub> inside the cell imbibing the aerogel is adjusted by a room-temperature gas handling unit. At the desired density, the sample is isolated from the gas handling unit with a room-temperature valve. There are three optical windows in the sample chamber, two are collinear and are used for the incidence and forward (transmitted) beams; the third is used to guide the beam that is scattered 90° from the forward direction. The forward intensity  $I_f$  from a 8 mW He-Ne laser is measured with a photodiode operating in the linear regime.

In order to determine the light scattering properties of our aerogel sample without fluid, we made an ancillary room-temperature experiment, in air, on a piece of aerogel that is shaped into similar dimensions as those in the sample cell. This is necessary since the piece of aerogel in the sample cells is, due to multiple windows and pinholes, inaccessible for visual inspection. In the room-temperature experiment, the laser beam is found to be well defined both inside and in the forward direction after it leaves the aerogel. Because of its cylindrical shape, the aerogel acts as a lens and the transmitted beams show divergence at distances beyond 10 cm from the aerogel sample. A larger sample, with a path length of 3 cm, and with flat surfaces is used to determine the attenuation of light inside the aerogel. The intensity of the laser beam is

found to decrease by 7% per cm path length, consistent with a recent measurement on aerogel of similar porosity [11].

The  $I_f$  result is shown in Fig. 1. For  $T \geq 140$  K,  $I_f$  saturates to a value (which we defined as 1) that is indistinguishable from that measured when there is no  $N_2$  in the sample cell. A rapid decrease in  $I_f$  is seen as  $T$  is lowered towards 125.37 K. It is natural to interpret this as a result of enhanced scattering due to strong density fluctuations, i.e., critical opalescence. An important difference from the usual critical opalescence of a pure fluid is that, instead of low intensity only near  $T_c$ ,  $I_f$  stays low as the temperature is reduced below 125.37 K, at least down to 113 K, the lowest temperature investigated. This does not appear to be a transient effect due to quick quenching since  $I_f$  stays at a low value at a fixed temperature for at least three days. The break in  $I_f$  vs  $T$ , which can be located to within 50 mK, is taken to be the boundary separating the one- and two-phase regions (see inset of Fig. 1). Figure 2 is a plot of the coexistence boundary located via this procedure applied to  $N_2$  fluid of different densities. The coexistence region as determined by vapor pressure isotherm measurements [8] at 124.2 and 125.25 K is found to be in good agreement with that determined via  $I_f$ . The liquid-vapor phase separation observed in this experiment differs from that of a pure fluid in that the low density "vapor" phase here consists of the vapor and a liquid film that adheres to the random silica strands. The low  $I_f$  indicates that the linear dimension of the domains of the "vapor" and liquid phases remain to be on the order of the wavelength of light but not of macroscopic size throughout the entire two-phase coexistence region.

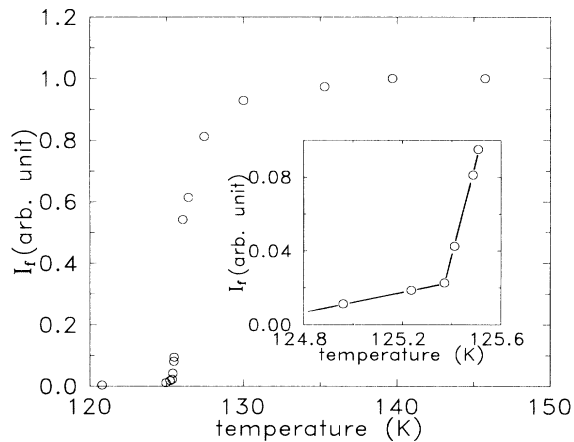


FIG. 1. Forward light intensity  $I_f$  vs temperature of  $N_2$  in aerogel at an average density of  $0.33 \text{ g/cm}^3$ . The inset shows linear extrapolations of  $I_f$  near the critical point, allowing for the determination of  $T_c$  (125.37 K). Similar breaks are seen at the temperature of the coexistence boundary at different densities of  $N_2$ .

The curve in Fig. 2 is a fit of the coexistence boundary by the form

$$\frac{\rho_{l,g} - \rho_{v,g}}{\rho_{c,g}} = B \left[ \frac{T_{c,g} - T}{T_{c,g}} \right]^\beta \quad (1)$$

$\rho_{c,g}$ ,  $\rho_{l,g}$ , and  $\rho_{v,g}$  are, respectively, the critical, liquid, and vapor densities of nitrogen in aerogel. The fitting parameters are  $B = 1.183 \pm 0.15$ ,  $\rho_c = 0.33 \pm 0.005 \text{ g/cm}^3$ ,  $\beta = 0.35 \pm 0.05$ , and  $T_{c,g} = 124.37 \pm 0.07 \text{ K}$ . The critical temperature of  $N_2$  in aerogel,  $T_{c,g}$  is 0.84 K below that of bulk  $N_2$ . If  $N_2$  in aerogel is indeed an experimental realization of the RFIM system, then  $T_{c,g} = T_{c,R}$ . The value of  $B$ , which characterizes the width of the coexistence region, is roughly 2.6 times smaller than that found for pure  $N_2$  without aerogel [12]. As noted above for  $^4\text{He}$  in aerogel, the value of  $\beta$  here is again consistent with that found for bulk fluid. It is interesting to note that in a recent x-ray synchrotron study, long-range order and a bulklike  $\beta$  were also found in another RFIM system, a dilute antiferromagnet,  $\text{Mn}_{0.75}\text{Zn}_{0.25}\text{F}_2$  [13].

The  $90^\circ$  scattered light, of intensity  $I(t)$ , with  $t$  denoting time, is brought through two pinholes, 40 cm apart to the photomultiplier tube, and the conditional signal is fed to a Langley Ford 1096 correlator. These pinholes of 0.1 and 0.05 cm diam are used to pick out light from a single coherence area. What is measured in our experiment is the time varying part of the intensity autocorrelation function  $G(\tau)$ ,

$$G(\tau) = \frac{\langle [I(t+\tau)I(t)] - \langle I \rangle^2 \rangle}{\langle I \rangle^2} \quad (2)$$

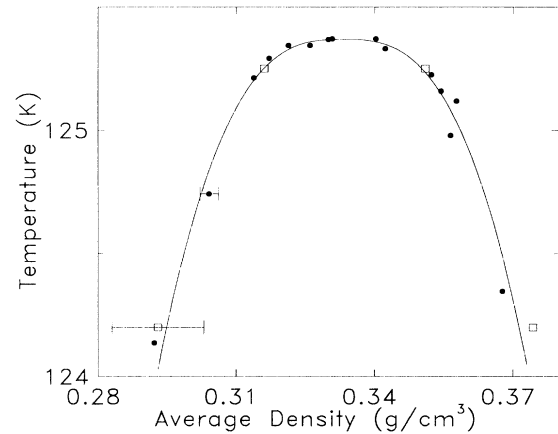


FIG. 2. The liquid-vapor coexistence boundary of  $N_2$  in aerogel. Solid circles and open squares show  $I_f$  and vapor pressure isotherm measurements, respectively. Typical uncertainties of these two measurements are also shown. The solid line is the best fit of the data (see text). Since the density of the first solid layer of  $N_2$  on the silica network is more than twice that of fluid  $N_2$ , the density of  $N_2$  participating in the transition can be (5-6)% lower than the average values shown, bringing better consistency in the value found for  $\rho_c$  here with that of pure  $N_2$  at  $0.31 \text{ g/cm}^3$ .

The angular brackets denote an ensemble average.

For most random signals, including all critical point fluids and particles undergoing Brownian motion,  $G(\tau)$  is proportional to the square of the dynamic structure factor,  $f_q(\tau) = \langle \rho_q(t+\tau)\rho_q(t) \rangle / \langle |\rho_q(\tau)|^2 \rangle$  [14]. In the above expression,  $\rho_q(t)$  is the  $q$ th Fourier component of the density, with  $q = (4n\pi/\lambda)\sin(\theta/2)$ . Here  $n$  is the refractive index of  $N_2$  fluid,  $\lambda$  is the vacuum wavelength (633 nm), and  $\theta = 90^\circ$  is the scattering angle. In a porous sample, however,  $G(\tau)$  is no longer proportional to  $|f_q(\tau)|^2$ . The reason is that the strong contribution to the scattered light from the rigid and random  $SiO_2$  structure in aerogel provides an unmodulated reference beam for the dynamic fluctuations, and one is in the so-called heterodyne limit [14]. In this limit  $G(\tau)$  is proportional to  $f_q(\tau)$ .

$G(\tau)$  was measured along an isochore near  $\rho_c$  at 0.33 g/cm<sup>3</sup> at a number of temperatures above and below  $T_{c,g}$ . Since multiple scattering effects may mask the true  $G(\tau)$ , we shall concentrate the discussion on  $G(\tau)$  results obtained under conditions where multiple scattering effects are clearly unimportant. In Fig. 3,  $G(\tau)$  at reduced temperature  $\epsilon = (T - T_{c,g})/T_{c,g} = 10^{-2}$  and  $8 \times 10^{-2}$  are shown in different scales. We are certain that there is very little multiple scattering effects at these temperatures because the transmitted intensities  $I_f$  at  $\epsilon = 10^{-2}$  ( $T = 126.62$  K) and  $\epsilon = 8 \times 10^{-2}$  ( $T = 135.4$  K), as shown in Fig. 2, are respectively 0.64 and 0.97 [15].

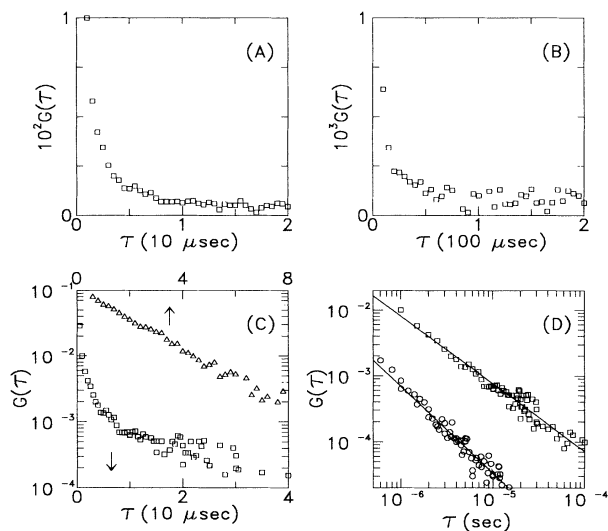


FIG. 3. Intensity autocorrelation function  $G(\tau)$  in the one-phase region. In panels (a) and (b) the correlator was set at two different sample increments and hence span different time ranges. Panel (c) shows semilogarithmic plots of  $G(\tau)$  for bulk  $N_2$  at  $\epsilon = 10^{-4}$  (triangles) and  $N_2$  in aerogel at  $\epsilon = 10^{-2}$  (squares). Panel (d) is a log-log plot for  $\epsilon = 10^{-2}$  (upper curve of squares) and  $8 \times 10^{-2}$  (lower curve of circles). The solid lines are the best fits to the data.

Figures 3(a) and 3(b) show  $G(\tau)$  vs  $\tau$  at  $\epsilon = 10^{-2}$  using sampling times of the correlator that differ by a factor of 10. In spite of the low signal-to-noise ratio in Fig. 3(b) [due to small  $G(\tau)$ ], these two figures are similar in shape and indicate the presence of slow decay in  $G(\tau)$ . The upper curve in Fig. 3(c) shows a log-linear plot of  $G(\tau)$  vs  $\tau$  for  $N_2$  near the critical density and at  $\epsilon = 10^{-4}$ , in the same sample cell, but with the aerogel removed. The observed exponential decay is expected. The lower curve in Fig. 3(c) is the same set of data shown in Figs. 3(a) and 3(b) for  $\epsilon = 10^{-2}$ . This set of data is presented to reaffirm that the decay of  $G(\tau)$  in aerogel is distinctly nonexponential. In contrast, a log-log plot as shown in Fig. 3(d) shows a reasonable description of  $G(\tau)$ , indicating power-law-like dependence of the form  $G(\tau) \sim A\tau^{-\phi}$  at  $\epsilon = 10^{-2}$  (upper curve). Note that a power-law-like dependence is also seen at a reduced temperature of  $8 \times 10^{-2}$  [lower curve, Fig. 3(d)], albeit only over one decade in time, between 1 and 10  $\mu$ sec. For  $\tau > 10$   $\mu$ sec,  $G(\tau)$  is swamped by the uncorrelated scattered light. The small value of  $G(\tau)$  for both  $\epsilon = 10^{-2}$  and at  $8 \times 10^{-2}$  at  $\tau = 1$   $\mu$ sec besides indicating a strong scattering for the rigid gel structure (i.e., heterodyne scattering), may also reflect a substantial decay of  $G(\tau)$  well inside 1  $\mu$ sec, the shortest resolving time of our correlator. Data gathered at  $\epsilon = 3 \times 10^{-2}$  are similar and fall between that at  $\epsilon = 10^{-2}$  and at  $\epsilon = 8 \times 10^{-2}$ .

Power-law dependence of  $G(\tau)$  on  $\tau$  is also seen at  $\epsilon = 10^{-3}$ ,  $3 \times 10^{-3}$ , and  $6 \times 10^{-3}$ . At these temperatures  $I_f$  is respectively, 0.09, 0.26, and 0.55, and the scattered light, particularly at  $\epsilon = 10^{-3}$  is expected to include a substantial fraction that has undergone multiple scatterings [15]. The slope of the power law, i.e., the value of  $\phi$ , increases monotonically with increasing temperature from  $0.8 \pm 0.1$  at  $\epsilon = 10^{-3}$  to  $1.2 \pm 0.1$  at  $\epsilon = 10^{-2}$  and  $1.4 \pm 0.1$  at  $\epsilon = 8 \times 10^{-2}$ . If the  $G(\tau)$  measurement is made under extreme multiple scattering limits,  $G(\tau)$  is likely to be distorted. In an earlier experiment with polystyrene spheres diffusing among strongly scattering 5  $\mu$ m immobile silica particles with  $I_f$  that is surely less than 0.01,  $G(\tau)$  is found to be proportional to  $1/\tau$  at large  $\tau$  [16]. We do not believe we are observing the same effect here since our results at temperatures above  $\epsilon = 10^{-2}$  should be virtually free of multiple scattering effects. The fact that a similar power-law dependence of  $G(\tau)$  on  $\tau$  is seen at  $\epsilon = 10^{-3}$  with  $I_f = 0.09$  is suggestive that the algebraic decay of  $G(\tau)$  is quite robust. The temperature-dependent  $\phi$  found in these measurements (rather than a  $\phi$  that stays at unity) is also supportive of a genuine power-law dependence of  $G(\tau)$  on  $\tau$ .

To assure that our result is free of nonergodic effects [17], we have made  $G(\tau)$  measurements while rocking the photomultiplier tube through an angle of  $2^\circ$ , at a rate of 50 sec per cycle to pick out light beams from different regions of the sample. No change in the power-law behavior of  $G(\tau)$  as shown in Fig. 3(d) is found.

One might expect to see a crossover from power law to bulklike exponential dependence for  $G(\tau)$  with increasing  $\epsilon$  as the correlation length in  $N_2$  is reduced to a value that is small compared with the "minimum" distance ( $\sim 10$  Å) between the  $SiO_2$  strands of the aerogel. The reason this is not seen is probably due to the fact that at large  $\epsilon$ , the  $1/e$  time of pure fluid  $N_2$  shrinks to a value that is too short to reveal the exponential form with our correlator. Based on Fig. 3(c), the  $1/e$  time at  $\epsilon = 8 \times 10^{-2}$  for pure  $N_2$  is about  $0.3 \mu\text{sec}$ , inside the resolving time of our apparatus of about  $1 \mu\text{sec}$ . As a consequence, only the long-time power-law tail of  $G(\tau)$ , reflecting the influence of aerogel, shows up between 1 and  $10 \mu\text{sec}$ .

In spite of the slow dynamics, we found no evidence of hysteresis in the coexistence boundary determined via  $I_f$ . Because of the large thermal masses, the time required to make each  $I_f$  and vapor isotherm measurement is on the order of 1000 to 3000 sec. It appears that at this time scale, which is at least  $10^{+6}$  times longer than that where activated dynamics is observed, the system has, in effect, reached equilibrium.

To conclude, whereas the nature of the equilibrium critical properties, at least in terms of the order-parameter exponent, are not changed, the dynamics or the decay of the density fluctuation for a fluid near criticality entrained in a piece of aerogel is dramatically altered.

We acknowledge instructive conversations with D. S. Cannell, D. S. Fisher, B. Frisken, J. S. Huang, D. A. Huse, A. J. Liu, J. Ma, J. Machta, A. Maritan, M. R. Swift, P. Wiltzius, X. L. Wu, and particularly J. R. Banavar. This work is supported by NSF under Grants No. DMR 9008461 (Penn State) and No. DMR 8914351 (Pittsburgh).

<sup>(a)</sup>Present address: AT&T Bell Laboratories, Murray Hill, NJ 07974.

- [1] S. B. Dierker and P. Wiltzius, *Phys. Rev. Lett.* **58**, 1865 (1987).
- [2] M. C. Goh, W. I. Goldberg, and C. M. Knobler, *Phys. Rev. Lett.* **58**, 1008 (1987).
- [3] J. V. Maher, W. I. Goldberg, D. W. Pohl, and M. Lanz, *Phys. Rev. Lett.* **53**, 60 (1984); K. Q. Xia and J. V. Maher, *Phys. Rev. A* **37**, 3626 (1988).
- [4] B. J. Frisken, F. Ferri, and D. S. Cannell, *Phys. Rev. Lett.* **66**, 2754 (1991); B. J. Frisken and D. S. Cannell, *Phys. Rev. Lett.* **69**, 632 (1992).
- [5] P. G. de Gennes, *J. Phys. Chem.* **88**, 6469 (1984).
- [6] A. J. Liu, D. J. Durian, E. Herbolzheimer, and S. A. Safran, *Phys. Rev. Lett.* **65**, 1897 (1990).
- [7] D. S. Fisher, G. M. Grinstein, and A. Khurana, *Phys. Today* **41**, No. 12, 56 (1988), and references therein.
- [8] A. P. Y. Wong and M. H. W. Chan, *Phys. Rev. Lett.* **65**, 2567 (1990).
- [9] A. T. Ogielski, *Phys. Rev. Lett.* **57**, 1252 (1986).
- [10] For a possible explanation for the non-RFIM exponent, see A. Maritan *et al.*, *Phys. Rev. Lett.* **67**, 1821 (1991).
- [11] P. H. Tewari, A. J. Hunt, and K. D. Lofftus, in *Aerogels*, edited by J. Fricke (Springer-Verlag, Berlin, 1985), p. 31.
- [12] M. W. Pestak and M. H. W. Chan, *Phys. Rev. B* **30**, 274 (1984).
- [13] J. P. Hill *et al.*, *Phys. Rev. Lett.* **66**, 3281 (1991); R. Birgeneau (private communication).
- [14] B. Chu, *Laser Light Scattering* (Academic, New York, 1991), Chap. III.
- [15] If the transmitted beam is reduced by a factor of  $e$  then the scattered photons on the average have undergone one scattering event.
- [16] P. Tong, W. Goldberg, and D. Pine (unpublished).
- [17] P. N. Pusey and W. Van Megan, *Physica* (Amsterdam) **157A**, 705 (1989); J. G. H. Joosten, E. T. F. Gelade, and P. N. Pusey, *Phys. Rev. A* **42**, 2161 (1990).